Lubna A. Jassim
Mohammed K. Jawad

Department of Physics, College of Science, University of Baghdad, Baghdad, IRAQ

Physical Properties of Natural Blend Thin Film Composites Reinforced with Nanoparticles

Solution casting technique was used to prepare polyvinyl alcohol/chitosan composite thin films with a total weight of 1g. Chitosan (Cs) and polyvinyl alcohol (PVA) blend was used as the natural matrix. Aluminum oxide (Al_2O_3) nanoparticles were added to the blend with different weight percentages (1, 1.5, 2, 2.5, and 3%). The effects of adding nano-Al_2O_3 on the physical properties of the prepared films, such as the microstructure, UV-visible and Fourier-transform infrared (FT-IR) spectra and x-ray differential (XRD) patterns, were studied. The experimental results indicated that the transmittance of all films do not vary greatly. According to the FTIR results, the optimum interaction between both polymers and nano-Al_2O_3 was observed at concentrations of 1% polymer mixed with nano-Al_2O_3 at 2.5 and 3 wt.%. Ultimately, the structural and physical characteristics of the films may be greatly enhanced by chitosan in a PVA blend with a concentration of 3% nano-Al_2O_3.

Keywords: Polyvinyl alcohol; Chitosan: Biopolymer; Inorganic nanoparticle
Received: 02 September 2023; **Revised:** 15 October 2023; **Accepted:** 22 October 2023

1. Introduction

Many synthetic polymers made from non-renewable fossil fuels have been and will continue to be in widespread use over the past decades. However, the production of these polymers not only leads to depletion of petroleum resources but also causes serious environmental pollution. Disposable products, especially materials used for short-term packaging, are slowly degraded in the environment, causing significant damage [1]. Most importantly related to the disposal of plastic waste is the operation of large landfills that can be used for other useful purposes such as agriculture [2]. These non-biodegradable polymers accumulate plastic waste and are eventually released into the environment in windy weather and eventually end up in the water. Therefore, if improperly disposed of, wildlife poses a danger to invade the environment in which the organism lives.

Fresh fruit needs to be coated with a non-toxic, ecologically friendly, durable and edible antimicrobial nanostructure to increase shelf life and maintain nutritional value [3-5]. Processing, procurement and transportation can all lead to bacterial contamination of the majority of our common fruits and vegetables [6]. Recyclability and environmental safety are becoming increasingly important in considering a better future for sustainability [7,8]. As a result, the demand for more flexible polymer-based materials has led to increase the interest in polymer composites filled with natural and organic fillers [9], such as biodegradable fillers. It is biodegradable and derived from renewable resources [10]. Biomaterials are becoming very important day by day for sustainable environmental development [11]. While biomaterials are being developed for drug delivery, tissue engineering and medical diagnostics. The physical and chemical methods by which reactions can be processed have improved significantly [12]. Chitosan is one of the most common natural polymers with linear polysaccharide structures is chitosan [13,14]. Furthermore, chitosan is an N-deacetylated chitin derivative with a high N-acetyl content. Chitosan has been widely used recently due to its industrial and biomedical applications [15]. Chitosan (CH) is a unique carbohydrate biopolymer produced by deacetylation (DA) of chitin, a major component extract from shellfish shells such as crabs, shrimps and crayfish. Chitin is the second most common natural biopolymer, behind the cellulose. The properties of chitosan can be significantly altered by undergoing physicochemical transformations such as mechanochemical disorganization, plasma treatment for amorphization and copolymerization [16,17]. In the same time, chitosan is not unique due to its low mechanical properties, such as other natural polymers which limit its applications [18]. Therefore, great efforts have been made to improve the mechanical properties and realize possible applications [19]. Blending is one of the most effective ways to deliver the new ingredients needed for film-forming applications [20].

PVA (polyvinyl alcohol) belongs to synthetic polymers for its better physical properties such as excellent oxygen barrier, flexibility, tensile strength, adhesion and suppression of fragrance release in the film [21,22]. Due to these excellent properties of PVA membranes are widespread used in biomedical applications [23]. Due to their ease of processing, low cost and excellent chemical properties, the nanomaterials have been developed and used in

various fields such as food, medicine and cosmetics [24]. Several studies have shown that nanomaterials can help improving polymer properties by incorporating polymers into nanomaterials such as and multi-walled carbon nanocomposites [25]. Aluminum oxide is one of the most widely used materials as a carrier in heterogeneous catalysts, adsorbents, electronics, abrasives and reinforcing ceramic composites because of its high strength, corrosion resistance, and high strength [26,27]. It is inexpensive and available in a variety of grades, making it suitable for many types of chemical reactions [28,29].

2. Materials and Methods

Polyvinyl alcohol (Mw from 85000 to 124000, DH= 99.8%), chitosan (medium molecular weight, 75–85% deacetylate), chemical weight $(C_2H_4O)_n$, chitosan chemical weight $(C_6H_{11}NO_4)_n$, and nano-aluminum oxide (Al_2O_3) with a particle size of 30±5 nm and purity of 98% were used.

Net polymers (Cs, PVA) and their mixtures at a fixed ratio of 1.5:1 and nanocomposite films were fabricated using a solution casting process. The primary PVA solution was fabricated by dissolving 0.6 g of PVA at 80°C in 8 ml of distilled water, while 0.4 g of Cs was dissolved in 20 ml of 1etic acid which heated to 50 °C and stirred for about 8 hours at 30°C. The mixture of PVA and Cs with a fixed ratio of 1.5:1 was fabricated by adding a soluble solution of Cs into the PVA solution dissolved for 24 hrs, using a magnetic stirrer. The solution was stirred continuously stir until a homogeneous aqueous solution is obtained. Nano-aluminum oxide mixed solution was fabricated using the same procedure maintained above. Polymer blends have been incorporated with various mass ratios of Al_2O_3 nanocomposites, (1, 1.5, 2, 2.5, and 3%) mass percent as listed in table (1). Finally, each mixed solution is poured onto the plate dish and left to dry. After 24 hrs, the film was dried and peeled off from the plate.

Table (1) Synthesis of Cs:PVA blend with introducing various ratios of nano-Al_2O_3

Sample	Polymer Name	Weight percentage (wt.%)	Nano-Al_2O_3 (%)
Cs	Chitosan	100	0%
PVA	Poly vinyl alcohol	100	0%
Ca: PVA	Chitosan: Polyvinyl alcohol	40:60	0%
A1	Chitosan: Polyvinyl alcohol	40:60	1%
A2	Chitosan: Polyvinyl alcohol	40:60	1.5%
A3	Chitosan: Polyvinyl alcohol	40:60	2%
A4	Chitosan: Polyvinyl alcohol	40:60	2.5%
A5	Chitosan: Polyvinyl alcohol	40:60	3%

Structural properties of samples was examined by Shimadzu 6000 X-ray Diffractometer with radiation source Cu (Kα) (λ=1.5405Å), 40 kV voltage and 30 mA current. The scan angle was varied from 2θ = 5° to 80° with speed of 5.00 deg/min. A ThermoScience Nicolet iN10 FTIR spectrometer was used to record the FTIR spectra within the range 400-4000 cm^{-1} in transmittance mode. Optical absorption spectra of all films were measured with Meterrech SP-8001 spectrophotometer within the range 300-1100 nm.

3. Results and Discussion

The crystalline structures of net PVA, chitosan and their mixture were introduced by XRD patterns as shown in Fig. (1). The characteristic chitosan peaks are concentrated at 11.9° and 18.6°, which are corresponding to diffraction planes of (020) and (110) for the orthorhombic structure, respectively, which agree with previous study [30]. The pure PVA exhibits two high peaks at 19.6424° and 23.2119° belonging to the (101) and (101) planes, respectively in addition to the weaker crystal peaks which agree with Sengwa et al. [30]. The XRD pattern of PVA:Cs shows wide peaks at 19.8609° and 11.5° corresponding to the presence of a new phase of chitosan due to the mixture. The main chitosan peak at 18.6225° was found to cross 19.8609°. These XRD peaks were observed to move towards lower and wider angle and reduced intensity compared with pure PVA samples. These results suggest the formation of PVA:Cs mixed by hydrogen bonding [31].

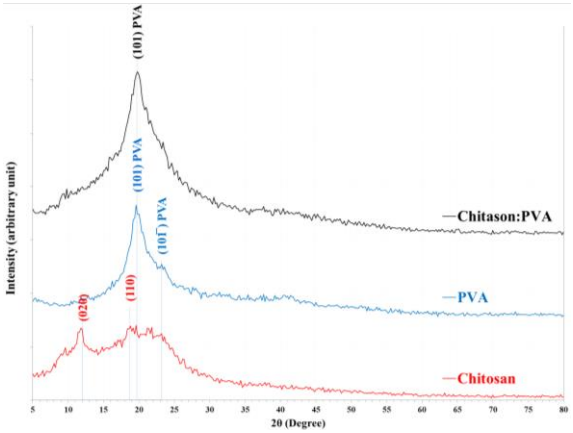

Fig. (1) XRD patterns of pure PVA, Cs and blend of PVA:Cs

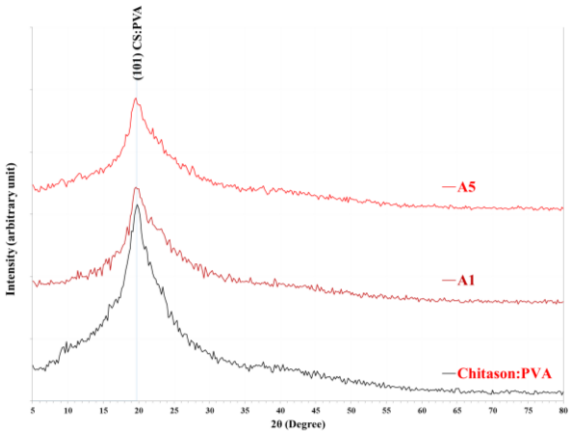

Fig. (2) XRD patterns of Cs:PVA mixture and nanocomposites (A1 and A5)

According to the XRD patterns of nanocomposite films filled with different weight percentages (1, 1.5, 2, 2.5 and 3%) of nano-aluminum oxide, a wide peak at 20° due to the polymer matrix is observed. However, the peaks are moving to 19.7059° and 19.6324° against Cs:PVA mixture, while FWHM increases with increasing the amount of nano-aluminum oxide.

FTIR is significant to determine and detect the specific structural properties and functional groups of polymers, which is sensitive to molecular changes in its structure. Various vertices of chitosan were found to originate at 3482.50 cm^{-1} indicating C–H stretching groups. At 1727.50 cm^{-1}, it exhibits stretching of C=O, amide II, and C–N stretchers. Peaks at 1570.00 cm^{-1} indicates -NH curvature and at 1146.25 cm^{-1} indicates amide III. The peaks 1420-1146 cm^{-1} indicate -C-O extensions of carboxyl groups. The FTIR spectrum of pure PVA shows the following broadband peaks. The peak at 3501.25 cm^{-1} is probably belonging to the OH segment, possibly due to interferences and intermolecular hydrogen bonding. The peaks at 2950 and 2908.78 cm^{-1} indicate vibrational curvature due to stretching of the C–H bond of the alkyl group. The peak at 1442.50 cm^{-1} represents the (OH)-C-OH bends of the amide group and the peaks from 1367.50 to 1123.75 cm^{-1} represent the -C-O segment of the carboxyl group. As shown in Fig. (3), the functional chemical groups in PVA include [32]. The absorption bands at 2950.00 and 2901.52 cm^{-1} belong to the CH_2 stretching vibration. The presence of a peak at 1723.75 cm^{-1} corresponds to the C=O extension of amide I and to the band at 1570.00 cm^{-1} for bending energy band in the N-H bond of the amine group. Small peak observed at 1123.75 cm^{-1} for C-O vibration. The wide peak at 1037.50 cm^{-1} corresponds to the C-O stretching oscillation connected by bone vibration peak at 842.50 cm^{-1} for C-H vibration [33].

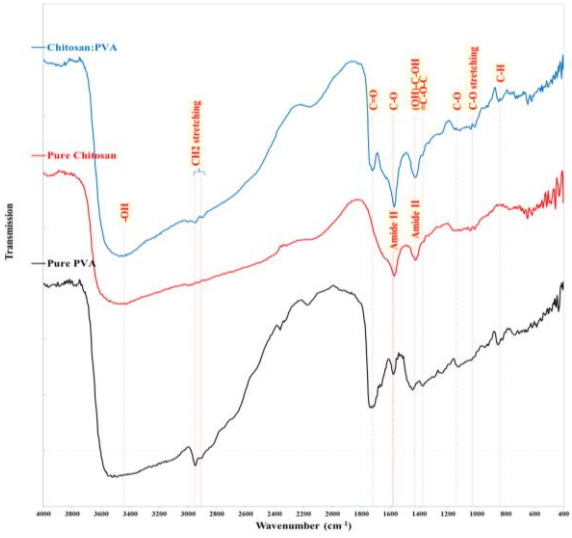

Fig. (3) FTIR spectra of pure PVA, Cs and the PVA:Cs mixture

Introducing of aluminum oxide with various ratios of (1, 1.5, 2, 2.5 and 3%) to the blend of Cs:PVA were displayed in Fig. (4). The peaks gradually increase change from 3467.50 to 3431.06, 3440.87, 3445.78, 3435.78 and 3453.12 cm^{-1} for O-H vibration. Compared with Cs:PVA mixture with introducing of nano-aluminum oxide leads to displacement or disappearance for some vertices. In comparison, the polymer blend of chitosan and PVA with introducing of nano-aluminum oxide, a peak occurs due to the interaction between intermolecular.

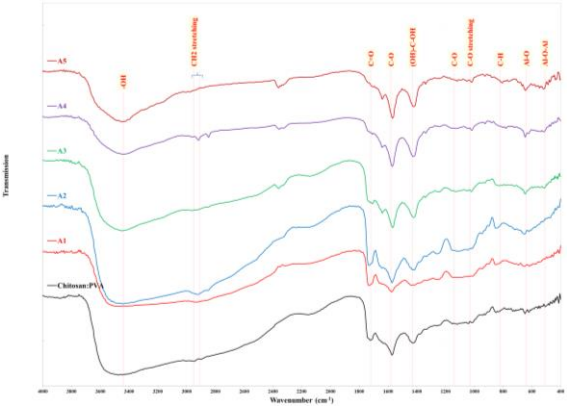

Fig. (4) FTIR spectra of polymers and nanocomposite mixture

The transmission spectra of the Cs:PVA nanocomposite films were recorded in the spectral range of 200-1100nm. The transmittance increases sharply within the UV region until a stability is reached in the visible and IR regions. In the UV range, the transmittance of Cs:PVA is higher than that of nano-aluminum oxide composite. This phenomenon is due to the higher nanocomposite content in the film [15]. The transmittance of all samples has decreased in the range 350-800nm. Although, no noticeable difference between the transmittance values of the samples was observed [34,35].

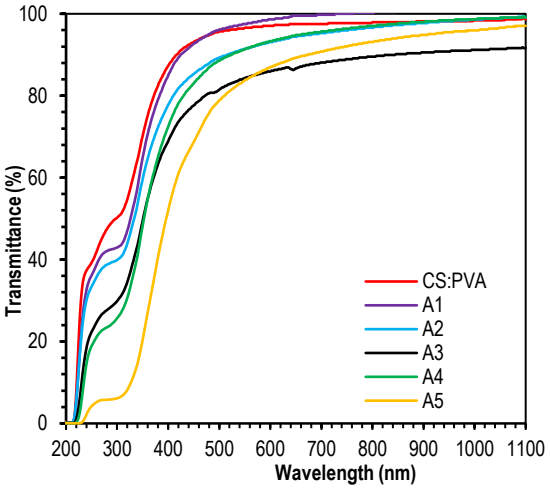

Fig. (5) Transmission spectra of PVA:Cs composite with different ratios of nano-Al_2O_3

The absorption edge for Cs:PVA mixture was found at about 230 nm as seen in Fig. (6). The absorption edges for Cs:PVA nanocomposites are slightly red-shifted towards long wavelengths. This may be due to the decrease in the energy level of the lowest uninhabited molecular orbital (LUMO) of PVA. The mixed Cs with PVA and the distance from the highest occupied molecular orbital (HOMO), will result in a red shift in the absorption spectrum. The results are consistent with Wang et al. (2016) and Nazeeruddin et al. (2003) that show an increase in the nano-Al_2O_3 ratio and the intensity reaches its maximum at 270nm as shown in Fig. (6).

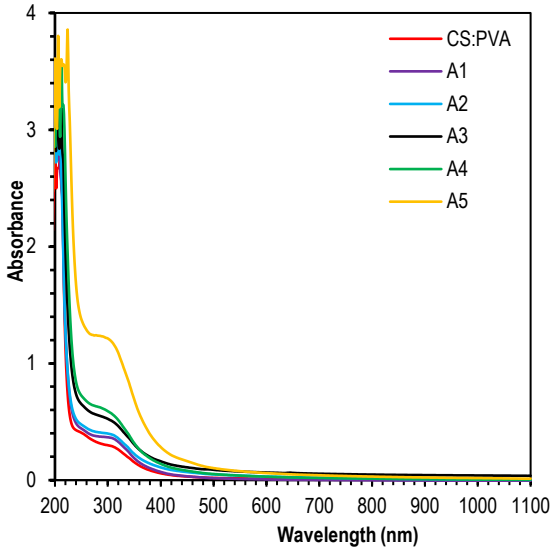

Fig. (6) Absorption spectra of PVA:Cs composite with different ratios of nano-Al_2O_3

Table (3) Variation of energy gap of the prepared thin films with nano-Al_2O_3 content

Sample	Energy band gap E_g (eV)
Cs:PVA	3.50
A1	3.45
A2	3.40
A3	3.40
A4	3.35
A5	3.35

The energy band gap of Cs:PVA mixture is calculated from Tauc's plot, to be 3.50 eV, and decreases with increasing weight percent of nano-aluminum oxide in the nanocomposites as explained in table (4). This may be due to the redshift of the adsorption spectra and it leads to decrease and narrow the energy band gap between HOMO and LUMO of nano-aluminum oxide composite. The decrease in the band gap is due to the increasing Al_2O_3 particle size, which can be attributed to the quantum size effect associated with nanoparticles, in agreement with Malliga et al. (2014). Figure (7) displays the variation of $(\alpha h\upsilon)^2$ as a function of photon energy ($h\upsilon$) for Cs:PVA blend and nano-Al_2O_3 with direct allowed transitions.

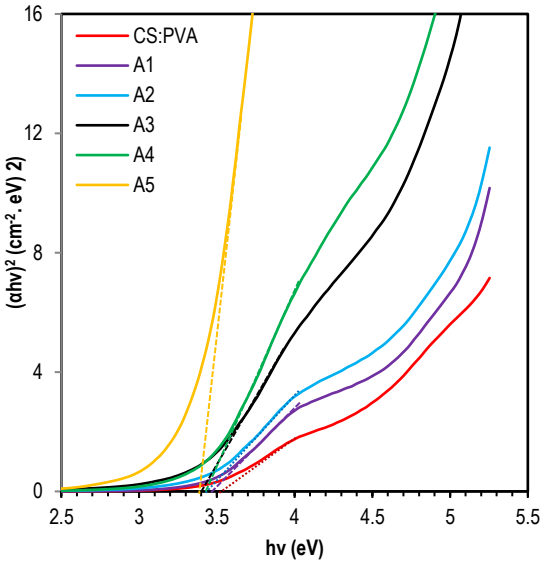

Fig. (7) Determination of energy band gap for PVA:Cs composite with different ratios of nano-Al_2O_3

4. Conclusions

According to the results obtained from this research, the physical properties of the polymer composites in presence of 3% Al_2O_3 nanoparticles were significantly modified. The amorphous structure of chitosan was revealed, which becomes much more crystalline when PVA is introduced. The structural characteristics of the nanocomposites filled with Al_2O_3 nanoparticles in the polymer matrix were enhanced. The variation of amounts of polymer and Al_2O_3 nanoparticles seem to be not significantly affecting the optical characteristics of the nanocomposite films.

References

[1] J. Cailloux et al., "Sheets of branched poly(lactic acid) obtained by one step reactive extrusion calendering process: Melt rheology analysis", *Express Polym. Lett.*, 7(3) (2013) 304-318.

[2] P. Ma et al., "Toughening of poly (lactic acid) by poly(β-hydroxybutyrate-co-β- hydroxyvalerate) with high β-hydroxyvalerate content", *Eur. Polym. J.*, 49 (2013) 1523-1531.

[3] S. Alamdari et al., "Green synthesis of multifunctional ZnO/chitosan Nano composite film using wild Mentha pulegium extract for packaging applications", *Surf. Interfaces*, 34 (2022) 102349.

[4] M. Ayub et al., "Nano materials as antimicrobial surface coatings: A parallel approach to restrain the expansion of COVID-19", *Surf. Interfaces*, 27 (2021) 101460.

[5] K.H. Le et al., "A novel antimicrobial ZnO nano particles added polysaccharide edible coating for the preservation of postharvest avocado

under ambient conditions", *Prog. Org. Coat.*, 158 (2021) 106339.
[6] X. Chen et al., "A smart chitosan nonwoven fabric coated with coumarin-based fluorophore for selective detection and efficient adsorption of mercury (II) in water", *Sens. Actuat. B: Chem.*, 342 (2021) 130064.
[7] D. Gomez-Maldonado et al., "Development of a β-cyclodextrinchitosan polymer as active coating for cellulosic surfaces and capturing of microcystin-LR", *Surf. Interfaces*, 33 (2022) 102192.
[8] R. Ahmad Ilyas et al., "Natural-Fiber-Reinforced Chitosan, Chitosan Blends and Their Nanocomposites for Various Advanced Applications", *Polymers*, 14 (2022) 874.
[9] S.M. Sapuan et al., "Mechanical Properties of Longitudinal Basalt/Woven-Glass-Fiber-reinforced Unsaturated Polyester-Resin Hybrid Composites", *Polymers*, 12 (2020) 2211.
[10] F.P. La Mantia and M. Morreale, "Green composites: A brief review. Compos", *Appl. Sci. Manuf. A*, 42 (2011) 579-588.
[11] S. Mitragotri and J. Lahann, "Physical approaches to biomaterial design", *Nat. Mater.*, 8 (2009) 15-23.
[12] R. Ilyas et al., "Polylactic Acid (PLA) "Biocomposite: Processing, Additive Manufacturing and Advanced Applications", *Polymers*, 13 (2021) 1326.
[13] S.K. Ramamoorthy, M. Skrifvars and A. Persson, "A Review of Natural Fibers Used in Biocomposites: Plant, Animal and Regenerated Cellulose Fibers", *Polym. Rev.*, 55 (2015) 107-162.
[14] J. Tarique et al., "Recent developments in sustainable arrowroot (*Maranta arundinacea Linn*) starch biopolymers, fibres, biopolymer composites and their potential industrial applications: A review", *J. Mater. Res. Technol.*, 13 (2021) 1191-1219.
[15] M. Kariminejad et al., "Chitosan/Polyvinyl Alcohol/SiO_2 Nanocomposite Films: Physicochemical and Structural Characterization", 12(3) (2022) 3725-3734.
[16] M.K. Jawad and N.K. Abid, "Study the effect of TiO_2 nanoparticles on physical properties of biopolymer blend", *IOP Conf. Ser.: Mater. Sci. Eng.*, 757 (2020) 012073.
[17] R. Priyadarshi and J.W. Rhim, "Chitosan-based biodegradable functional films for food packaging applications", *Innov. Food Sci. Emerg. Technol.*, 62 (2020) 102346.
[18] F. Garavand et al., "A comprehensive review on the Nano composites loaded with chitosan nanoparticles for food packaging", *Crit. Rev. Food Sci. Nutr.*, 62(5) (2020) 1383-1416.
[19] I.A. Neacsu et al., "Biomimetic Composite Scaffold Based on Naturally Derived Biomaterials", *Polymers*, 12 (2020) 1161.
[20] E. Podgorbunskikh et al., "Mechanical Amorphization of Chitosan with Different Molecular Weights", *Polymers*, 14 (2022) 4438.
[21] M. Aslam, M.A. Kalyar and Z.A. Raza, ''Polyvinyl Alcohol: A Review of Research Status and Use of Polyvinyl Alcohol Based Nano composites", 58(12) (2018) 2119-2132.
[22] S.B. Aziz et al., "The Study of Plasticized Amorphous Biopolymer Blend Electrolytes Based on Polyvinyl Alcohol (PVA):Chitosan with High Ion Conductivity for Energy Storage Electrical Double-Layer Capacitors (EDLC) Device Application", *Polymers*, 12(9) (2020) 1938.
[23] B.Y. Ahmed and S.O. Rashid, "Synthesis, characterization, and application of metal-free sulfonamide-vitamin C adduct to improve the optical properties of PVA polymer", Arab. J. Chem., 15(10) (2022) 104096.
[24] A.Z. Naser, I. Deiab and B.M. Darras, "Poly (lactic acid)(PLA) and polyhydroxyalkanoates (PHAs), green alternatives to petroleum-based plastics", *RSC Adv*., 11 (2020) 17151-17196.
[25] A.M. Abdelghany et al., "Experimental and DFT studies on the structural and optical properties of chitosan/polyvinyl pyrrolidone/ZnS nanocomposites", *Polym. Bull*., 80 (2023) 13279-13298.
[26] R. Romero Toledo et al., "Effect of aluminum precursor on physicochemical properties of Al_2O_3 by hydrolysis/precipitation method", *Nova Scientia*, 10(20) (2018) 83-99.
[27] A. Fathy and O. El-Kady, "Thermal expansion and thermal conductivity characteristics of Cu–Al_2O_3 nanocomposites", *Mater. Des.*, 46 (2013) 355-359.
[28] J. Ancheyta, M.S. Rana and E. Furimsky, "Hydroprocessing of heavy petroleum feeds: Tutorial", *Catalysis Today*, 109(1) (2005) 3-15.
[29] L. Boone et al., "Preparation and Characterization of Chitosan Obtained from Shells of Shrimp", *Mar. Drugs*, 15 (2017) 1-12.
[30] R.J. Sengwa, S. Choudhary and P. Dhatarwal, "Investigation of alumina nanofiller impact on the structural and dielectric properties of PEO/PMMA blend matrix-based polymer nanocomposites", *Adv. Compos. Hybrid Mater.*, 2(1) (2019) 162-175.
[31] M.I. Shariful et al., "Adsorption of divalent heavy metal ion by mesoporous-high surface area chitosan/poly(ethylene oxide) nanofibrous membrane", *Carbohydr. Polym.*, 157 (2017) 57-64.
[32] M. Akhlaq et al., "Methotrexate-Loaded Gelatin and Polyvinyl Alcohol (Gel/PVA) Hydrogel as a pH-Sensitive Matrix", *Polymers*, 13 (2021) 2300.
[33] S.R. Kanatt et al., "Active chitosan–polyvinyl alcohol films with natural extracts", *Food Hydrocolloids*, 29(2) (2012) 290-297.

[34] R. Mohammadi et al., "Physico-mechanical and structural properties of eggshell membrane gelatin-chitosan blend edible films", *Int. J. Biol. Macromol.*, 107 (2018) 406-412.
[35] S.F. Hosseini et al., "Preparation and functional properties of fish gelatin–chitosan blend edible films", *Food Chem*., 136 (2013) 1490-1495.
[36] P. Srinivasa et al., "Properties and sorption studies of chitosan–polyvinyl alcohol blend films", *Carbohydr. Polym.*, 53 (2003) 431-438.
[37] M.A. Saleh and M.K. Jawad, "Polypyrrole/Functionalized Multi-Walled Carbon Nanotube/Nickel Oxide Nanocomposites: Structural, Morphological, Optical and Composition Analysis Studies", *Nano Hybrids Compos.*, 35 (2022) 85-94.

Table (2) Typical PVA bands: composite Cs and nano-Al_2O_3

Band type	Chitosan :PVA blend	A-1	A-2	A-3	A-4	A-5
O-H	3467.50	3431.06	3440.87	3445.78	3435.97	3453.13
CH_2	2950.00 2901.25	2940.60 -	2925.95 2847.41	- -	2913.62 2847.41	1714.44 1640.87
C=O	1723.75	1731.61	1731.61	1709.54	1711.99	-
C-O	1570.00	1574.66	1772.21	1767.30	1772.21	1767.30
(OH)-C-OH	1423.75	1432.43	1415.26	1420.16	1422.62	1422.62
C-O	1123.75	-	-	-	1135.69	1118.53
C-O stretching	1037.50	-	1040.05	1020.44	1017.98	1015.53
C-H	842.50	848.77	848.77	-	787.47	804.63
Al-O	-	654.23	652.59	647.68	650.14	647.68
Al-O-Al	-	-	-	515.26	515.26	517.71

